JOURNAL OF MATERIALS SCIENCE 32 (1997) 4909–4916

Anodic film formation on high strength aluminium alloy FVS0812

J. SYKES, G. E. THOMPSON, D. MAYO*, P. SKELDON‡
* *British Aerospace Defence Limited, Warton, Preston, PR4 1AX, UK*
‡ *Corrosion and Protection Centre, UMIST, P.O. Box 88, Manchester M60 IQD, UK*

Barrier-type film growth on the high strength aluminium alloy FVS0812 has been studied by a combination of transmission electron microscopy and Rutherford backscattering spectroscopy. The film is composed mainly of amorphous anodic alumina, but is contaminated with iron species incorporated into the film from the alloy. The film may also be contaminated with silicon and vanadium species at levels below the detection limit of the present experiments. The contaminant species are primarily incorporated locally into the film during oxidation of $Al_{13}(Fe, V)_3Si$ dispersoids and the resulting film material is of reduced resistivity compared with anodic alumina of high purity. As a consequence of the presence of regions of film material of differing resistivities, the film is of irregular thickness. The average thickness corresponds to a nm/V ratio of about 1.3. Iron species incorporated into the film migrate outwards at roughly 2.1 times the rate of Al^{3+} ions. The iron species are not ejected in significant amounts to the electrolyte on reaching the film/electrolyte interface and hence, a thin layer of film material highly enriched in iron species develops at the film surface. The layer may also be enriched in vanadium species, if these are incorporated into the film and migrate more rapidly than Al^{3+} ions. Enrichment of iron, and possibly other alloying element atoms, is found in a thin layer of alloy immediately beneath the anodic film, paralleling enrichments of alloying element atoms found following anodic oxidation of other aluminium alloys. The enrichments at both the alloy/film and film/electrolyte interfaces do not appear to be continuous across the macroscopic surface of the specimens, probably due to the non-uniformity of film growth on the two-phase substrate. The maximum voltage for the selected conditions of anodizing was limited to 68 V as a result of oxygen generation at flaws which are present extensively in the anodic film.

1. Introduction

The aluminium alloy FVS0812 is a high strength, high temperature material, which is prepared by rapid solidification, comminution and powder metallurgy technology. The alloy properties, including retention of strength after exposure at 425 °C for 1000 h [1], result from a microstructure comprising about 27 vol % fine, spherical $Al_{13}(Fe,V)_3Si$ dispersoids in a relatively pure aluminium matrix [2]. In addition to the superior elevated-temperature strength and stability of the alloy, due to the relatively slow coarsening rate of the dispersoids, the corrosion resistance of alloy FVS0812 to salt fog exposure is better than the 2000 and 7000 series alloys. Such behaviour is related to the relatively inert role of the fine silicide dispersoid distribution. It is possible that the corrosion performance may be improved further by anodizing as well as providing porous anodic films over the macroscopic alloy surface for wear resistance and adhesive bonding. Initial studies, by other workers, of the anodizing of FVS0812, have focused on barrier film growth, revealing a relatively flawed anodic film compared with that formed on high purity aluminium [3]. From previous work on aluminium alloys, modified film growth is expected above second phase material [4].

Prior to investigation of the formation of porous anodic films, which are of practical relevance, further study of barrier film growth has been carried out in the present work in order to elucidate the oxidation of aluminium and alloying element atoms at the alloy/film interface and the subsequent migration of the respective ions in the anodic film. The use of barrier films facilitates detailed analyses owing to their greater thickness compared with the barrier layer at the base of the usual porous films, which is typically ~20 nm thick. This study complements earlier work [3] by investigating thicker barrier-type anodic films, using a combination of Rutherford backscattering spectroscopy (RBS) and transmission electron microscopy (TEM) in order to determine quantitatively both average (macroscopic) and local (microscopic) properties of the film across the surface of the alloy. The enrichment of iron atoms in a alloy layer of about 2 nm thickness immediately beneath the anodic film and the migration of iron ions in the anodic film at a faster rate than Al^{3+} ions, leading to accumulation

0022–2461

of iron ions in a thin layer of material at the film/electrolyte interface, are revealed.

2. Experimental procedure

2.1. Material and specimen preparation

Samples of the FVS0812 alloy (nominal composition 8.5 wt% (4.3 at%) Fe, 1.7 wt% (1.7 at%) Si, 1.3 wt% (0.7 at%) V) were mechanically polished using silicon carbide paper, to 1200 grit, and diamond paste, to 1 μm. Following masking with beeswax to define a working area of about 1 cm^2, individual specimens were anodized at 25 mA cm^{-2} in stirred 0.1 M ammonium hydrogen borate electrolyte at 293 K. The voltage response was monitored on a fast-response chart recorder.

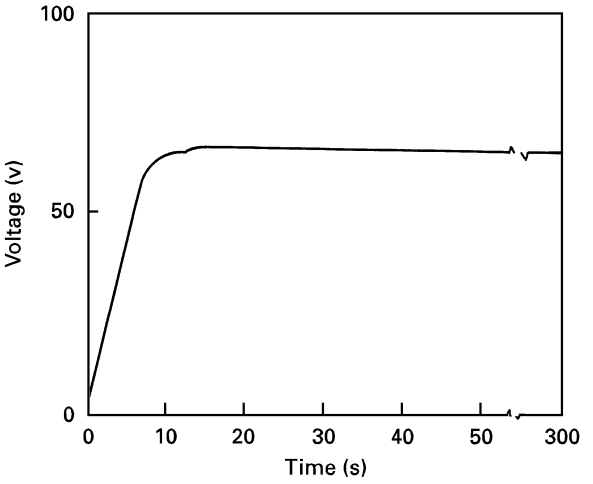

Figure 1 Voltage-time response for anodizing FVS0812 alloy at 25 mA cm^{-2} in 0.1 M ammonium hydrogen borate electrolyte at 293 K.

2.2. Specimen examination

Sections, about 10 nm in thickness, of the anodized specimens, prepared by ultramicrotomy [5], were examined in a JEOL FX 2000 II transmission electron microscope equipped with energy-dispersive X-ray (EDX) analysis facilities. A nominally 20 nm diameter electron probe was used for the analyses, providing sufficient spatial resolution and X-ray count rate. Specimens were also examined by RBS using 2.0 MeV alpha particles supplied by the Van de Graaff accelerator of the University of Paris. The beam current and diameter were about 60 nA and 0.5 mm respectively. Alpha particles were detected at 150° to the incident beam direction. Data were analysed by the RUMP program [6] with scaling of the stopping power of oxygen by 0.88 [7].

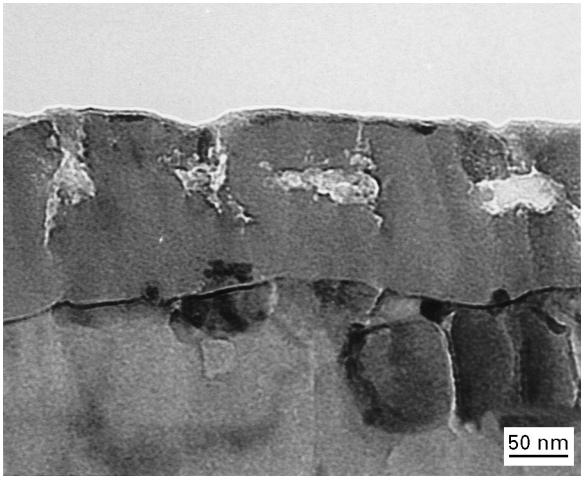

Figure 2 Ultramicrotomed section of FVS0812 alloy, anodized at 25 mA cm^{-2} to 68 V in 0.1 M ammonium hydrogen borate electrolyte at 293 K, revealing flaws and non uniform film thickness.

3. Results

3.1. Voltage–time response

The voltage–time response for anodizing at a constant current density of 25 mA cm^{-2} in 0.1 M ammonium hydrogen borate solution was initially linear with a slope of 8.0 ± 0.2 V s^{-1} to about 60 V (Fig. 1). At this latter voltage, the slope diminished to a relatively low value and the voltage approached a plateau level of about 68 V. Following the change in slope, copious gas evolution was observed at the surface of the specimen. In the approach to the plateau level, the ionic current density in the film decays to practically zero.

3.2. Transmission electron microscopy

An ultramicrotomed section of the specimen anodized under the standard conditions for 5 min to a voltage of 68 V (Fig. 2) reveals a barrier-type anodic film, of non-uniform thickness, attached to the alloy substrate. The alloy substrate contains dispersoids of about 50–100 nm in diameter. The composition of the dispersoids, by EDX, was consistent with the expected $Al_{13}(FeV)_3Si$ [1]. The matrix material was composed of relatively pure aluminium (> 99.4%). The dispersoids were generally distributed homogeneously in the alloy but clusters were evident in some regions. Measurements of the anodic film thickness at positions along several different ultramicrotomed sections indicated an average thickness of about 88 nm, a maximum thickness of 120 nm and a minimum thickness of 61 nm. From the anodizing voltage, namely 68 V, average, maximum and minimum nm/V ratios of 1.30, 1.76 and 0.90 are suggested. For film growth on high purity aluminium under the selected conditions, but without ionic current decay, the nm/V ratio is about 1.17 [8], about 10% less than the above average value for the alloy.

The anodic film contains a significant number of flaws, revealed in Fig. 2, located near to the middle of the film section. Flaws can function as immobile markers within anodic films formed on high purity aluminium and their presence at a depth of 40%, and possibly more, of the film thickness is indicative of film growth at high Faradaic efficiency [9]. Their presence at about this position in the films on the present alloy suggests that film growth proceeds without significant loss of Al^{3+} ions to the electrolyte [9], which is expected for film growth in the selected borate electrolyte [8]. Thus, the reduced efficiency of film growth,

from the voltage–time response, is associated mainly with oxygen evolution at flaws in the anodic film. Further, the films show no significant hydration of film material at the film/electrolyte interface.

The general appearance of the film material remote from flaws (Fig. 3) is typical of amorphous anodic alumina. Notably, at some regions of the film/electrolyte interface, a thin layer, about 2–5 nm thick, of much darker appearance is evident. Later analyses reveal that this layer is highly enriched in iron ions compared with the average composition of the film. Inspection of the alloy/film interface, discloses areas at which oxidation of dispersoids had taken place prior to the termination of anodizing. Above these dispersoids, the anodic film material is similar in appearance to that above adjacent areas at which oxidation of the matrix was previously taking place. The dimensions of the dispersoids are similar to the anodic film thickness. Importantly, RBS analysis of the mechanically polished alloy revealed the bulk composition to the alloy surface, indicating that pull-out of dispersoids during polishing does not occur to any significant extent. Thus, at some areas of the mechanically polished, original surface of the alloy, the film is developed by oxidation of dispersoid material exclusively, whilst at some other areas oxidation of matrix material occurs. Elsewhere, film growth involves sequential oxidation of both matrix and dispersoid material. Where remnants of large dispersoids, or clusters of dispersoids, are present at the alloy/film interface, suggesting mainly oxidation of dispersoid material in growth of the overlying anodic film, the film is locally thicker than the average thickness (Fig. 4). However, it is not possible to identify by direct observation of the film material, discrete regions of film material associated with oxidation of either matrix or dispersoid material exclusively, since there is no direct evidence, from contrast, of iron-enriched and iron-depleted regions of the main film.

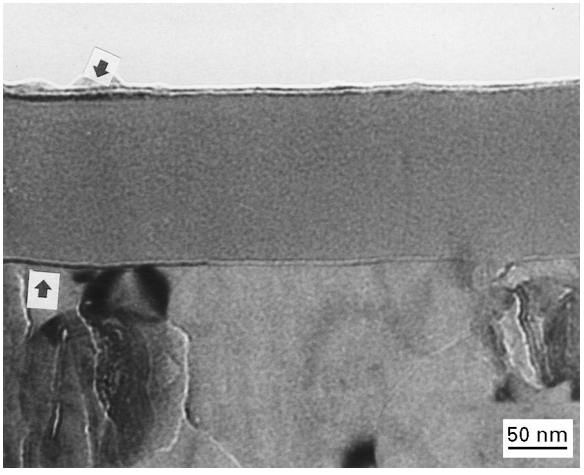

Figure 3 Ultramicrotomed section of the FVS0812 alloy, anodized at 25 mA cm^{-2} to 68 V in 0.1 M ammonium hydrogen borate electrolyte at 293 K, revealing a layer of alloy enriched in iron just beneath the anodic film and a layer of film material enriched in iron species at the film/electrolyte interface. The enriched layers are indicated by arrows.

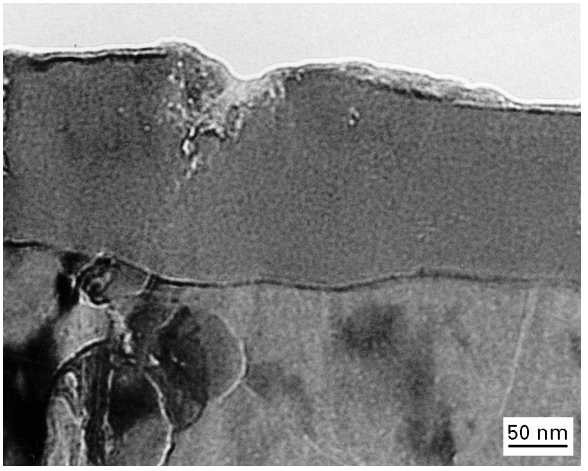

Figure 4 Ultramicrotomed section of the FVS0812 alloy, anodized at 25 mA cm^{-2} to 68 V in 0.1 M ammonium hydrogen borate electrolyte at 293 K, revealing thicker film material above dispersoids.

EDX analyses were carried out at several points near the middle of the anodic film (Fig. 5a), which indicated the presence of iron species incorporated into the film from the alloy. Any vanadium and silicon species present were below the detection limits. Analyses at different points along the mid-thickness of the film, revealed significant variation in the atomic ratio of iron to aluminium due to the incorporation of iron species into the film primarily from discrete dispersoids. Examples of analyses, given in Table I, reveal Fe/Al ratios of 0.02–0.11. The average ratio of iron to aluminium in the main film, from analyses at five separate locations, was about 5×10^{-2}. Analysis of the enriched layer of film material at the film/electrolyte interface (Fig. 5b) revealed an increased concentration of iron, with a typical Fe/Al ratio of 0.2–0.4, but precise analysis of the layer is not possible due to the small thickness of the layer compared with the diameter of the electron probe, nominally 20 nm.

At regions of the alloy/film interface, a fine alloy layer, of about 1–2 nm thickness, can be observed which is significantly darker than the adjacent alloy (Fig. 3). The layer, presumed to be iron-rich, is present in association with both matrix and dispersoid material, but primarily the latter. The thickness of the layer is much less than the diameter of the electron probe available for EDX analysis and, additionally, the layer is usually associated with dispersoid material of high iron content; thus, accurate analysis of the composition of the layer was not possible.

3.3. Rutherford backscattering spectroscopy

The experimental spectrum of alpha particles elastically scattered from the alloy, anodized for 5 min to 68 V, was typical of that of a mainly alumina film attached to an aluminium alloy substrate (Fig. 6a). The mass difference between iron and vanadium is sufficient to determine the distribution of iron species through most of the anodic film thickness. Thus, the energy range associated with scattering from iron species in the anodic film is of most interest in the spectrum (Fig. 6b). The concentrations and distributions

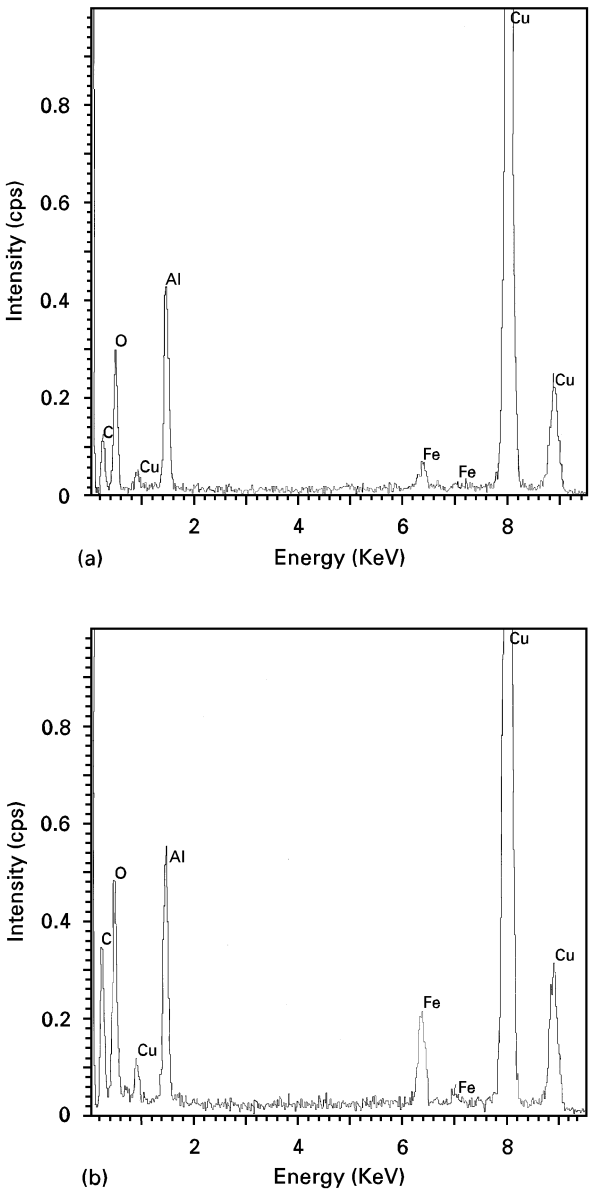

Figure 5 Typical EDX spectrum measured (a) at the mid-thickness of the anodic film and (b) at the enriched layer at the anodic film surface for the FVS0812 alloy, anodized at 25 mA cm^{-2} to 68 V in 0.1 M ammonium hydrogen borate electrolyte at 293 K.

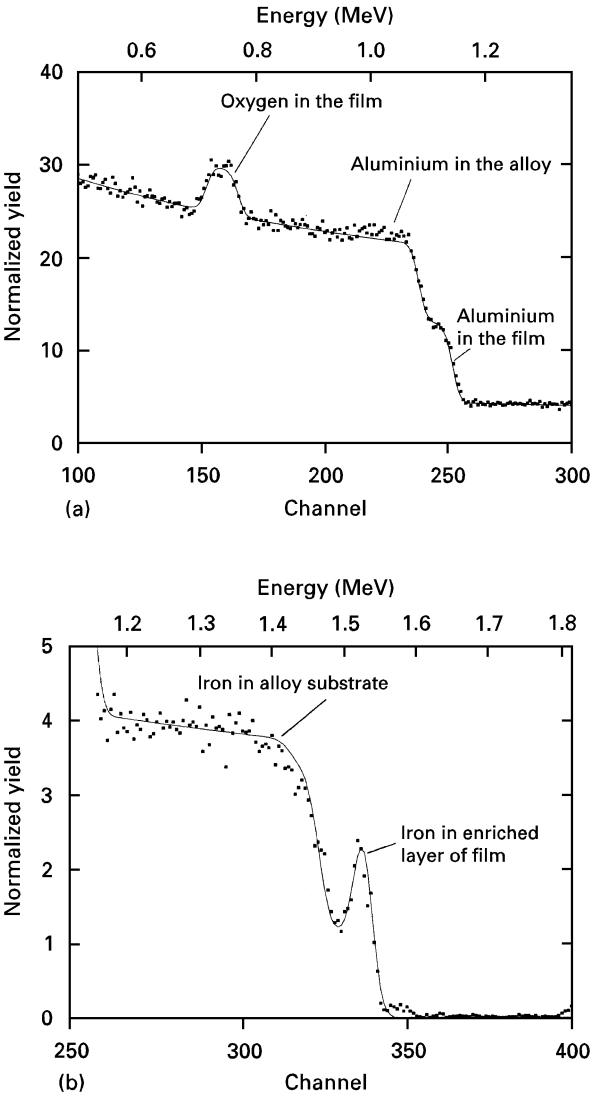

Figure 6 (a) Simulated and experimental RBS spectra for the FVS 0812 alloy, anodized at 25 mA cm^{-2} to 68 V in 0.1 M ammonium hydrogen borate electrolyte at 293 K. (b) Details of region showing elastic scattering from iron.

TABLE 1 EDX analyses at the mid-thickness of the anodic film on FVS0812 alloy formed at 25 mA cm^{-2} in 0.1 M ammonium hydrogen borate electrolyte at 293K

Analysis	Atomic ratio Fe/Al
1	0.06
2	0.11
3	0.02
4	0.03
5	0.04

of silicon and vanadium species, which are the minor alloying elements, are not determined since their relatively low yields are not resolved from yields due to aluminium ions in the film and iron atoms in the alloy, respectively.

The simulation giving best agreement with the experimental data indicated 5.0 at % Fe in the alloy. The concentrations of silicon and vanadium in the alloy were presumed to correspond with the nominal composition of the alloy of 1.7 and 0.7 at % respectively. The most notable feature of the experimental spectrum is a sharp peak at the energy corresponding to alpha particles scattered from iron nuclei at, or close to, the film surface. The peak suggests an iron-enriched surface layer containing about 9.0×10^{15} iron ions cm^{-2}, to an accuracy of about 20%. The thickness of the layer is less than the depth resolution of the technique. However, good agreement with the experimental spectrum can be obtained by assuming a thickness of 2.5 nm, which is typical of the thickness of the iron-enriched layer directly evident by TEM. The measured enrichment is an average across the analysed area, namely about 2.5×10^{-3} cm^2.

The experimental spectrum also indicated the presence of iron species within the bulk of the anodic film. The simulation indicated an average Fe/Al atomic ratio of about 3.5×10^{-2} through the film, in reasonable agreement with EDX. The limited depth resolution precluded a precise analysis of the distribution of

iron species through the film thickness. Any yield due to the possible presence of vanadium species in the enriched layer at the surface of the film occurs in the same energy range as that from iron species near the alloy/film interface. Thus, the measured Fe/Al ratio is possibly an upper limit if some contribution to the experimental yield is made by vanadium species.

The simulation revealed an average film thickness of 92 nm, in good agreement with that found by TEM, assuming a film composed essentially of anodic alumina, of density about 3.2 $g\,cm^{-3}$, with an Fe/Al ratio given previously. The edge corresponding to scattering from iron nuclei in the alloy at the alloy/film interface was significantly broadened due to the non-uniformity of the film thickness. As a result of the varying thickness, the presence of iron enrichment of the alloy, suggested by TEM, could not be confirmed. The film contains about 2.0×10^{16} iron ions cm^{-2}, made up of 9.0×10^{15} iron ions cm^{-2} in the thin enriched layer at the film surface and, from the average thickness and average composition of the main film, 1.1×10^{16} iron ions cm^{-2} in the film bulk.

4. Discussion

The TEM results reveal the formation of a barrier film on the FVS0812 alloy with a non-uniform thickness. The average nm/V ratio, 1.30, is about 10% greater than that expected for anodic alumina grown under the selected conditions but without current decay. The higher average nm/V ratio is explained by the reduced film resistivity, mainly due to the incorporation of iron species, and the decay of ionic current with concomitantly reduced field in the region of the approach to the voltage plateau in the voltage–time response. The non-uniform thickness results from the heterogeneity of the substrate which comprises about 27 vol % $Al_{13}(Fe,V)_3Si$ dispersoids in a relatively pure aluminium matrix. Previous work has demonstrated anodic film growth on Al_3Fe at a nm/V ratio of about 2.0, significantly higher than that for usual anodic alumina [4]. Thus, the presence of iron species in the anodic film [4] reduces the ionic resistivity of the film. Film growth on the $Al_{13}(Fe,V)_3Si$ dispersoids is expected to approximate to that on Al_3Fe, with possible modifications if significant incorporation of silicon and vanadium species into the film occurs. On present evidence, the resistivity of the film material above the dispersoids is greater than that above Al_3Fe, since the maximum nm/V ratio for the FVS0812 alloy is about 1.8 rather than 2.0. This lower nm/V ratio is compatible with a reduced concentration of iron in the second phase.

Evidence from unpublished work of the authors on film growth on Al– Si alloys suggests incorporation of a low concentration of silicon species into anodic alumina does not reduce significantly the film resistivity. Further, silicon species are immobile in anodic alumina films and hence, if incorporated from an alloy substrate, are expected to contaminate only the material of the inner $\sim 60\%$ of the film thickness which is formed at the alloy/film interface by inward migration of O^2/OH^- ions [10]. Vanadium species, if incorporated into the film, are probably of minor importance since they represent of the order of only 15% of the total transition metal species. Based on a previous study of the migration of implanted vanadium ions [11], the vanadium species probably migrate faster than Al^{3+} ions. Hence, vanadium species may be present both in the film bulk and, if they are not ejected under the field to the electrolyte, in the enriched layer of film material at the film/electrolyte interface.

As a consequence of the differing resistivities of film material above the dispersoid and matrix material of the substrate, the current density across the alloy/film interface is non-uniform during film growth. Thus, initially, current flows preferentially through the lower resistivity film material that grows above the dispersoids which are exposed at the original mechanically polished surface. On sufficient local thickening, the current re-distributes as the resistance of the film above the dispersoids approaches that of the film above the matrix. Resulting from the approximately uniform distribution of the dispersoids in the matrix, the current continues to vary locally as matrix and dispersoid materials are intercepted sequentially by the retreating alloy/film interface. Thus, a film develops with relatively rough, on a nanometre scale, alloy/film and film/electrolyte interfaces.

The non-uniformity of film growth on the alloy may assist cracking of the film due to stresses generated by formation of film material in constrained volumes and geometrical changes at the alloy/film interfaces. Such cracks will be healed rapidly by local formation of new film material, which will further roughen the film interfaces. The location of flaws in the film suggests that growth of the film occurs by migration of Al^{3+} ions outward and O^{2-}/OH^- ions inward resulting in formation of approximately similar amounts of film material at the film/electrolyte and metal/film interfaces respectively. For film growth on high purity aluminium at high efficiency, about 40 and 60% of the film material is formed at the film/electrolyte and metal/film interfaces, respectively [12]. Thus, as discussed later, the film on the alloy grows without significant loss of Al^{3+} ions to the electrolyte.

The initial slope of the voltage–time response, namely 8.0 $V\,s^{-1}$, can be compared with that expected for growth of high purity anodic alumina at high Faradaic efficiency for the selected conditions of anodizing, namely about 12 $V\,s^{-1}$. The significantly reduced slope suggests that the film on the alloy develops at about 70% efficiency in the initial stage of anodizing. The low efficiency is probably due mainly to evolution of oxygen at flaws in the film. Evidently, film growth on the alloy practically ceases above about 68 V due to the consumption of almost all of the current by oxygen evolution under a high voltage. In comparison, film growth on high purity aluminium in the selected electrolyte is sustained to voltages in excess of 300 V, being limited essentially by dielectric breakdown. As a consequence of the significance of oxygen evolution, the average ionic current density through the film material is less than the total current density of 25 mA cm^{-2}, and will diminish as oxygen

evolution makes a progressively greater contribution to the total current. In the present work, the flaws in the anodic film have not been studied systematically, since the main interest is in formation of alumina film material. Hence, the processes determining the development of flaws and the contribution of oxygen evolution to the total current are not elucidated here. The variation in the average ionic current density with progress of anodizing is not considered to be of major importance to interpretation of the mechanism of general film growth, which for anodic alumina films is relatively independent of the current density over a wide range [13]. This independence is associated with the co-operative nature of ionic transport in amorphous anodic films [14].

The key results from RBS are the findings of iron species in the anodic film generally and the enrichment of iron species in a thin layer of film material at the film/electrolyte interface. The analysis lacks the spatial resolution, both laterally, in the plane of the specimen surface, and in depth, normal to the specimen surface, needed to provide precise local compositions of the film material. However, the analysis complements the TEM, which determines film composition in highly localized regions of the specimen surface, by providing details of average compositions over a relatively wide area. As discussed earlier, the films reveal significant variability in local composition and thickness, because of the influence of second phase material on film growth. Further, TEM discloses the presence of a thin layer of alloy immediately beneath the anodic film that is highly enriched in iron, and possibly also vanadium and silicon, compared with the composition of the bulk alloy. This enriched alloy layer, which is discontinuous along the alloy/film interface, is not detected by RBS, due to the non-uniformity in thickness of the film.

From work on the anodic oxidation of dilute binary aluminium alloys, oxidation of the alloying element at the alloy/film interface follows the establishment of a thin layer of alloy underneath the film that is sufficiently enriched in the alloying element [15]. The enrichment is developed by prior oxidation of aluminium that occurs in the early stages of the film growth when an essentially pure alumina film is formed. Subsequent to the establishment of the enriched layer, atoms of both aluminium and the alloying element are oxidized at the alloy/film interface, in their alloy proportions, throughout further anodizing. For the present alloy, the behaviour is initially presumed to be similar to that expected for a binary Al–Fe alloy; the possible effects of silicon and vanadium, present in lower concentrations than iron, are returned to later. The following discussion proceeds on the assumptions that the film and substrate are uniform across the specimen surface and that the necessary enrichment of iron in the alloy at the alloy/film interface is present at the commencement of anodizing. These assumptions are subsequently justified.

For most dilute aluminium alloys, oxidation of atoms of the alloying element at the alloy/film interface results in an ion species in the film which migrates outwards at a rate u relative to Al^{3+} ions, where u is the ratio of the migration rate of the metal ion species to the migration rate of Al^{3+} ions. Consequently, the ratio, R, of the concentration of the ion species of the alloying element in the film (considering cations only) to the corresponding concentration of the alloying element in the alloy is given by [15]:

$$R = \frac{1}{(0.6 + 0.4u)} \tag{1}$$

For the present alloy, RBS indicates that for iron $R \approx 0.7$, and hence $u \approx 2.1$. Evidently the reduced concentration of iron in the film compared with the alloy is caused by the significantly faster migration rate of iron ions compared with Al^{3+} ions. Faster migration rates of alloy element ions, compared with Al^{3+} ions, are also found for a wide range of other metal ions in anodic alumina, including copper [16] and zinc [17] species. When the alloying element ions migrate faster than Al^{3+} ions, a layer of film material can develop at the outer film surface which is highly enriched in associated metal oxide; for example, unpublished work of the authors reveals a layer of samaria at the film/electrolyte interface in anodic films grown at high Faradaic efficiency on Al-Sm alloys. For the investigated specimen, anodized to 68V, an average thickness of film material of about 90 nm is formed. Accordingly, using a Pilling-Bedworth ratio of about 1.61 for anodic alumina [18], about 56 nm of alloy are consumed by oxidation; the oxidized layer of alloy contained about 1.7×10^{16} iron atoms cm^2. The detection of about 2.0×10^{16} iron ions cm^{-2} in the anodic film suggests that iron species incorporated into the film at the alloy/film interface, which migrate outward at a faster rate than Al^{3+} ions, are not ejected to the electrolyte at the film/electrolyte interface.

According to the previous analysis, the behaviour of iron during anodic oxidation of the FVS0812 alloy can be explained by the immediate oxidation of both iron and aluminium atoms in their alloy proportions, at the alloy/film interface, followed by the outward migration of both cations, with a migration rate of iron ions about 2.1 times that of Al^{3+} ions. At the present time, the precise oxidation state of iron in the film is not known. The faster migration of iron ions results in a layer of film material enriched in iron species at the film/electrolyte interface. The preceding analysis, which is based upon the assumption that the film material is developed without ejection of Al^{3+} ions to the electrolyte, is supported by the observation of flaws, apparent as voids in micrographs, at about 40% of the film thickness. The latter depth separates regions of film material formed by migration of Al^{3+} ions outwards from that formed by migration of O^{2-}/OH^- ions inward, for growth at high Faradaic efficiency. The reduced efficiency of anodizing is therefore caused primarily by oxygen evolution at particular sites on the alloy surface, but is not due to significant loss of Al^{3+} ions to the electrolyte.

The assumption that iron ions are incorporated into the film formed on the FVS0812 alloy immediately upon the commencement of anodizing is consistent with the behaviour observed in homogeneous Al-5

at % W alloys. For the latter, the period of prior oxidation of aluminium is complete at an anodizing voltage of about 3 V [19]. Moreover, for the present alloy, the period of prior oxidation of aluminium is essentially eliminated since the iron atoms are contained mainly within second phase particles containing about 20 at% Fe. At such high concentrations, the necessary enrichment of the alloy in iron for oxidation of iron to proceed is achieved practically immediately upon commencement of anodizing, as assumed in the model. Regions between second phase material, which contain relatively little iron, can be disregarded in the present analysis, since the necessary enrichments of iron in the alloy for oxidation of iron atoms to proceed are not possible during oxidation to voltages of 68 V.

In certain regions across the alloy surface, during anodic oxidation of the estimated average thickness of about 56 nm of alloy, both second phase and matrix material are consumed. If the matrix material is oxidized initially, as occurs when the matrix phase is above the second phase material at the region of interest, the low concentration of iron in the matrix merely accumulates in the alloy at the alloy/film interface during oxidation of the matrix layer, but without significant oxidation of iron atoms. Subsequently when the alloy/film interface encroaches upon the underlying dispersoids, the necessary accumulation of iron atoms is achieved rapidly and, for practical purposes, iron and aluminium atoms are then oxidized in their dispersoid proportions. However, since iron ions are not incorporated into the film during the previous oxidation of the matrix phase, the iron ions derived from the second phase material, subsequently incorporated into the film, may not have time to migrate significantly across the film thickness. The local distribution of iron ions in the film obviously depends upon the depth of matrix material that is initially oxidized locally, prior to oxidation of the dispersoid material. Conversely, if dispersoid material is oxidized first, iron ions are incorporated essentially immediately into the film and continue to be incorporated until the second phase particle is consumed. Subsequently effectively no further oxidation of iron atoms occurs until the alloy/film interface encroaches a deeper lying second phase particle. The composition of the film locally, on a nanometre scale therefore varies significantly both across the surface of the specimen and in depth, according to locations at which no dispersoid material has been oxidized, and hence no iron ions have been incorporated into the film, to the other extreme of locations at which only second phase material has been oxidized and hence the film is highly contaminated by iron ions. At the latter regions, from Equation 1, the average concentration of iron ions in the bulk of the film material is estimated to be comparatively high, on average about 15% of the total cations; an example of a measured concentration approaching this level is given in Table I.

The outer 40% of the thickness of films grown at high efficiency in borate is normally contaminated by boron species which are incorporated into the film at the film/electrolyte interface [10]. The boron species, present at a low concentration, are immobile in the film under the electric field. In the films on FVS0812 alloy, boron species are presumably incorporated into film material grown above the matrix phase which is essentially high purity aluminium. Whether boron species are incorporated into film material developed above the dispersoid phase is uncertain; at these regions the layer of film material highly enriched in iron and vanadium species may inhibit incorporation of boron species.

5. Conclusions

1. Barrier-type anodic films formed on FVS0812 at 25 mA cm^{-2} in a borate electrolyte are composed of amorphous alumina which is contaminated by iron species, and possibly vanadium and silicon species, incorporated into the film material from the alloy. Resulting from the heterogeneity of the substrate, with the alloying elements mainly contained within the dispersoid phase, the composition of the film reveals significant local variations on a scale of a few nanometres.

2. The films form at an average nm/V ratio of about 1.3. However, the thickness of the film reveals significant local variations associated with the differing resistivities of film material formed above dispersoid and matrix phases of the substrate.

3. The iron species incorporated into the film at the alloy/film interface migrate outwards in the film at about 2.1 times the rate of Al^{3+} ions. On reaching the film/electrolyte interface the iron species are not ejected to the electrolyte to any significant extent and hence, a layer of film material is present adjacent to the film/electrolyte interface which is highly enriched in iron species. As a consequence of the faster migration of iron species, compared with Al^{3+} ions, the bulk of the film is depleted in iron in comparison with the alloy composition. Vanadium and silicon species, if present in the films, are below the detection limits of the present analysis. On the basis of previous work, it is likely that vanadium and silicon species in the film migrate outward and are immobile, respectively.

4. At areas of the alloy/film interface, thin layers of alloy, about 2 nm thick, are present which are highly enriched in iron and possibly silicon and vanadium. The enrichment, developed by prior oxidation of aluminium, is essential for oxidation of iron and other alloying elements to occur.

5. The film forms at reduced Faradaic efficiency due to evolution of oxygen at the specimen surface. Oxygen evolution, associated with relatively extensive flaws in the film, limits film growth to a maximum anodizing voltage of 68 V corresponding to a film of about 90 nm average thickness.

Acknowledgements

The authors acknowledge the industrial support of BAe (Military Aircraft) in this work; thanks are also given to Professor G. Amsel and Dr C. Ortega for provision of time on the Van de Graaff accelerator at the University of Paris (work partially supported by

Centre National de la Recherche Scientifique (GDR86)).

References

1. M. S. ZEDALIS, D. RAYBOULD, D. J. SKINNER and S. K. DAS, in: "Processing of Structural Metals by Rapid Solidification", Orlando, Florida, 6–9 Oct., 1986, edited by F. H. Froes and S. J. Savage, (American Society for Metals, Ohio, 1987) p. 347.
2. P. S. GILMAN, *Metals and Mater.* **8** (1990) 504.
3. S. C. THOMAS, V. I. BIRSS, D. STEELE and D. TESSIER, *Microscopy Research and Technique* **31** (1995) 285.
4. K. SHIMIZU, G. E. THOMPSON, G. C. WOOD and K. KOBAYASHI, *J. Mater. Sci. Lett.* **10** (1991) 709.
5. R. C. FURNEAUX, G. E. THOMPSON and G. C. WOOD, *Corros. Sci.* **18** (1978) 853.
6. L. R. DOOLITTLE, *Nucl. Instrum. Meth.* **B 15** (1986) 227.
7. J. C. CHEANG WONG, JIAN LI, C. ORTEGA, J. SIEJKA, G. VIZKELETHY and Y. LEMAITRE, *ibid.* **B 64** (1992) 169.
8. A. C. HARKNESS and L. YOUNG, *Can. J. Chem.* **44** (1966) 2409.
9. K. SHIMIZU, G. E. THOMPSON and G. C. WOOD, *Phil. Mag.* **B 64** (1991) 345.
10. G. C. WOOD, P. SKELDON, G. E. THOMPSON and K. SHIMIZU, *J Electrochem. Soc.* **143** (1996) 74.
11. W. D. MACKINTOSH, F. BROWN and H. H. PLATTNER, *ibid.* **121** (1974) 1281.
12. F. BROWN and W. D. MACKINTOSH, *ibid* **120** (1973) 1096.
13. L. YOUNG and D. J SMITH, *ibid* **126** (1979) 765.
14. G. E. THOMPSON, Y. XU, P. SKELDON, K SHIMIZU, S. H. HAN and G. C. WOOD, *Phil. Mag.* **B 55** (1987) 651.
15. H. HABAZAKI, K. SHIMIZU, P. SKELDON, G. E. THOMPSON and G. C. WOOD, *ibid* **B 74** (1996) 443.
16. H. HABAZAKI, M. A. PAEZ, K. SHIMIZU, P. SKELDON, G. E. THOMPSON, G. C. WOOD and X. ZHOU, *Surf. Interface Anal.* **23** (1995) 892.
17. X. ZHOU, H. HABAZAKI, K. SHIMIZU, P. SKELDON, G. E. THOMPSON and G. C. WOOD, Corros. Sci. **38** (1996) 1563.
18. J. P. S. PRINGLE, Electrochim. Acta **25** (1980) 1423.
19. H. HABAZAKI, K. SHIMIZU, P. SKELDON, G. E. THOMPSON and G. C. WOOD, *J. Electrochem. Soc.* **143** (1996) 2465.

Received 7 march 1996
and accepted 7 April 1997